Analysis of mobilized stress ratio of gap-graded granular materials in direct shear state considering coarse fraction effect

By

X. S. Shi

Professor, 1. Key Lab of Ministry of Education for Geomechanics and Embankment Engineering, Hohai University, Nanjing, China

2. Department of Civil and Environmental Engineering,

The Hong Kong University of Science and Technology, Hong Kong.

Email: qingsongsaint@gmail.com; xiusongshi@hhu.edu.cn

Kai Liu (Corresponding author)

Doctoral student, Department of Civil and Environmental Engineering,

The Hong Kong Polytechnic University, Hung Hom, Kowloon, Hong Kong, China

Email: kevin-kai.liu@connect.polyu.hk

Jianhua Yin

Professor, Department of Civil and Environmental Engineering,

The Hong Kong Polytechnic University, Hung Hom, Kowloon, Hong Kong, China

Email: cejhyin@polyu.edu.hk

Apr. 2020

Abstract

Weathered rockfill materials, characterized by a mixture of soil matrix and rock aggregates, are widely distributed in mountainous areas. These soils are frequently used for subgrade or riprap in engineering practice, and the mobilized shear strength is crucial for analyzing the displacement and stability of these geo-structures. A series of direct shear tests are performed on a gap-graded soil with a full range of coarse fraction. The behavior of gap-graded soils is analyzed, and a simple model is proposed for the evolution of mobilized stress ratio during direct shearing process based on mixture theory. The change of inter-aggregate configuration is incorporated by introducing a structure variable which increases with coarse fraction and decreases approximately linearly with the overall horizontal shear strain in double logarithmic plot. It reasonably reflects a gradually transformation from a matrix-sustained structure into an aggregate-sustained one with the increase of coarse fraction. The model has four parameters, and at least two direct shear tests need to be done for the calibration. Validation of the model is done by using the test data in this work and those from literature.

Keywords: Direct shear tests; Mobilized stress ratio; Gap-graded soils; mixture theory; Volume average scheme

1. Introduction

Weathered rockfill materials are distributed worldwide, especially in mountainous areas (Yang and Juo, 2001; Zhao *et al.*, 2007; Peters and Berney, 2010; Zhou *et al*., 2016; Qin and Chian, 2017; Wei *et al*., 2018). For example, Chongqing soil from western China (Chen *et al.*, 2020b) is a typical weathered gap-graded soil. The particle size between 0.425 mm and 2.0 mm is missing, and it can be characterized by a mixture of fines and rock aggregates. The fine matrix can be either originated from a weather induced disintegration or a tectonic deformation of weak rock (Chandler, 2000; Ruggeri *et al*., 2016; Peng et al., 2018; Shi *et al*., 2019; Guo and Cui, 2020). Gap-graded soils are frequently used for subgrade or riprap in engineering practice, since they can be obtained locally (Vallejo, 2001; Chang *et al*., 2014; Chen *et al*., 2020a; Meng et al., 2019; Tan et al., 2019). The shear strength of gap-graded soils is crucial for analyzing the stability of these geo-structures.

The shear strength of gap-graded soils has been investigated by many researchers (e.g., Kumar and Wood, 1999; Yin, 1999b; Vallejo and Mawby, 2000; Simoni and Houlsby, 2006; Shin and Santamarina, 2012; Ruggeri *et al*., 2016). They reported that the fraction of aggregates has a considerable influence on the shear strength, which is related to the internal structure of gap-graded soils. Thevanayagametal and his colleagues (Thevanayagam and Mohan, 2000; Thevanayagametal et al., 2002) presented a schematic interpretation for the structural evolution of fine-coarse mixtures, and it provides a useful reference for analyzing the compressibility and shear behavior of gap-graded granular soils. Micromechanics based models (Chang and Yin, 2011; Yin et al., 2014; Chang et al., 2017), equivalent void concept (Thevanayagam et al., 2002; Thevanayagam and Martin, 2002; Yin et al., 2016), and mixture theory (Shi et al., 2019; Shi et al., 2020) are used to evaluate and capture the coarse fraction effect of gap-graded soils.

The ultimate shear strength of the gap-graded soils was fully analyzed based on direct shear

tests by previous researchers (e.g., Vallejo and Mawby, 2000; Yagiz, 2001; Simoni and Houlsby, 2006; Ruggeri et al., 2016; Zhou *et al*., 2016). However, design approaches based on ultimate shear strength fail to reflect realistic transition of soils from the initial state to the final failure state (Bolton *et al*., 1990a and 1990b). To this end, Bolton *et al*. (1990a, 1990b, 2008) and Osman and Bolton (2004, 2006) suggested that mobilized shear strength should be used to assess the safety and to compute deformations in vicinity of retaining systems.

Mobilized shear strength relies on the mobilized stress ratio defined as the ratio of the shear stress to the vertical stress in direct shear tests. In this work, we present several points which were not reported by others: (1) gap-graded soils with a prescribed void ratio of matrix are tested, so that the coarse fraction effect can be assessed; (2) a new homogenization law is proposed for the stress ratio of gap-graded mixtures, which couples the overall stress ratio with that of the matrix; (3) a simple model is proposed for the evolution of the stress ratio with only two state variables. Experimental data from literature is also adopted for a further validation.

2. Materials and test scheme

Materials

Chongqing soil consists of two different size of components, termed as coarse aggregates and fine matrix. Most of the soil particles with a size between 0.425mm and 2.0mm were missing, indicating that the Chongqing soil is a typical gap-graded soil. The fine soil matrix is obtained by sieving Chongqing soil through a mesh opening of 0.425 mm. The particle size distribution curve of the fine soil does not follow the fractal limiting grading curve:

$$P(d) = 100 \times \left(\frac{d}{d_{\max}} \right)^n \tag{1}$$

where $P(d)$ is the cumulative percentage passing the sieve, d_{max} is the maximum size of particles, and n is a constant parameter. The particle size distribution of the fine matrix in Chongqing soil is not consistent with Eq. (1), since the fines are originated from weathering factors (e.g., seasonal temperate and humidity oscillations). The density of fine soil particles is 2.73 Mg/m^3. The maximum and minimum void ratios of the fine matrix are 1.323 and 0.406, respectively. The optimum moisture content is 12%, and the corresponding maximum dry density is 1.94 Mg/m^3.

The typical sizes distinguishing the aggregates and the matrix vary according to the degrees of rock mass weathering. E.g., for the Chongqing soils, the typical sizes are 0.425mm and 2mm. Particles between these two limit values are missing, and soil particles larger than 2.0 mm are categorized as coarse aggregates. Since the test data may be not reliable for very coarse granular materials in direct shear tests, a coarse sand material from Hong Kong (denoted as HK sand) is used to replace the rock aggregates in Chongqing soil. The density of sand particle is 2.63 Mg/m^3. To distinguish the coarse fraction effect, only the coarse particles (HK sand) with a size between 1.13 mm and 2.0 mm are used as inclusions. The ratio of representative particle size (e.g., D_{50}) between aggregates and fines is ca. 8. This type of mixtures shows a distinct coarse fraction effect, and it can be categorized as a typical gap-graded soils (Ueda et al., 2011). Most of the coarse particles in HK sand have a subangular to angular shape. The basic physical properties of the matrix and aggregates are given in Table 1 (BS 1377). The minimum void ratio $e_{min,a}$ and maximum void ratio $e_{max,a}$ of HK sand are 0.60 and 0.95, respectively.

Test scheme

The test apparatus utilized in this work is a modified direct shear system (Borana *et al*. 2016). The stainless-steel shear box has a diameter of 10 cm and a height of 4 cm. It is well

recognized that the overall behavior relies on both coarse fraction and behavior of the soil matrix. The objective of this study is to evaluate and model the coarse fraction effect. To this end, the state of soil matrix of mixtures should be the same. E.g., the moisture content and the initial void ratio of the soil matrix. In this study, an optimum water content (12%) is adopted for the matrix. Six different coarse fractions are considered in this study (0%, 20%, 40%, 55%, 80%, 100%, The "coarse fraction" denotes the mass fraction of coarse aggregates, which differs from the "volume fraction of coarse aggregates").

To produce gap-graded soils, the fine soil matrix and the coarse aggregates were mixed homogeneously for a visual homogeneity at room conditions. Then, the mixtures are matured in an airtight container for several hours for a uniform distribution of moisture content. After finishing the direct shear test, the mixtures from three different parts of a specimen are sampled (top, bottom and the middle in vicinity of the shear plane). The coarse fraction and moist content are measured, and most of the data are approximately close to the desired values, with a relative error less than 4%. The particles size distribution curves of the mixtures with various coarse fractions are shown in Fig. 1.

It is fully recognized that the initial state of soils has a significant influence on the shear strength (e.g., Chandler, 2000; Yao *et al*., 2004; Yao *et al*., 2009; Hong *et al*., 2012; Shi and Yin, 2018; Zhou *et al*., 2016). Therefore, the initial void ratio of the fine matrix in mixture samples (coarse fraction below 73%) should be the same, otherwise, one cannot distinguish the effect of coarse fraction and the initial void ratio of the matrix. The desired dry density of the fine matrix is 1.61 Mg/m^3 in this study. If it is assumed that the fine matrix and the coarse aggregates are fully mixed, the overall void ratio of the mixture can be computed, as shown in Fig. 2. ('fully mixed' means an ideal mixing process: when the fraction of fines is higher than the porosity of the coarse aggregates, the coarse grains float in a fine matrix. Otherwise, all fines are confined within the inter-aggregate space.) The overall void ratio decreases as the

coarse fraction increases, and it is formulated as a function of the void ratio of fine matrix e_m and the coarse fraction ψ_a:

$$e = e_m(1-\psi_a) \tag{2}$$

Note that Eq. (2) is only suitable for matrix-sustained structure as shown in Fig. 3, i.e., most of the coarse aggregates float within a fine matrix. The overall void ratio decreases until it approaches the transitional point (the lowest point in Fig. 2), ($e = \tilde{e}$, and $\psi_a = \tilde{\psi}_a$, see Appendix-1 for details). This point corresponds to the transitional structure in Fig. 3. With a further increase of coarse fraction, the overall void ratio increases, and aggregate-sustained structure forms. The "ideal compaction" line can be expressed as

$$e = (1+e_a)\psi_a - 1 \tag{3}$$

where e_a is the void ratio of coarse aggregates. The overall void ratio of the mixture after compaction is shown in Fig. 2 (solid diamond points). It is seen that the "ideal compaction" state can be achieved in case of lower coarse fractions (0%, 20%, 40% and 55%). However, the data point of the mixture with 80% coarse fraction is located above the ideal state, this corresponds to the loose structure beyond the "transitional coarse fraction" in Fig. 3. A possible interpretation is that fine particles of matrix are accommodated between coarse aggregates during preparation, denoted as the "wedging effect". As described in Fig. 3, the fine particles separate adjacent aggregates from each other and participate in force chains. As a result, the coarse aggregates are prevented from forming an ideal dense structure. This phenomenon has been observed by Goudarzy et al. (2016) using micro-CT scanning.

All the specimens are prepared using a moist tamping technique. Different compaction methods were utilized to prepare the specimen according to the coarse fraction: for a high coarse fraction (80% and 100%), the specimen cannot hold itself after being extruded from a mold. Therefore, it was directly compacted inside the shear box in 4 layers using a vibrating

hammer (each layer has a height of 1.0 cm after compaction). For a lower coarse fraction (0%, 20%, 40% and 55%), the volume of matrix is high enough to sustain the coarse aggregates. The specimen was slightly compacted inside a square mold using a vibrating hammer in 4 layers. The top surface of the layers was scratched after compaction to guarantee the homogeneity of the soil specimen. Finally, the specimen was extruded from the mold to the shear box for a further consolidation and shearing.

An initial stress of 4.7 kPa was applied to the specimens. It was increase to 157-451 kPa by gradually adding weights to the loading hanger, following the steps of 19.6, 39.3, 78.5, 157, 314, and 451 kPa. Finally, the specimens were sheared under a constant vertical stress (157 kPa, 314 kPa, and 451kPa) at a displacement rate of 0.02 mm/min. The shear tests were stopped if the horizontal shear strain reaches 15% or the asymptotic state is approached.

3. Test results and discussions

The fraction of coarse aggregates is independent of state of mixtures; therefore, it is not a good choice for analyzing the mechanical behavior of gap-graded mixtures. As an alternative, the volume fraction of the coarse aggregates ϕ_a is adopted for the compressibility of lumpy soils and sand-clay mixtures (Shi and Yin, 2017; Shi et al., 2020). It varies due to different compressibility of the two constituents. It can be approximated by the overall void ratio and the coarse fraction (see Appendix-1):

$$\phi_a = \frac{\psi_a}{1+e} \tag{4}$$

where e is the overall void ratio, ψ_a is the coarse fraction of gap-graded soils. Eq. (2) and Eq. (4) incorporate the assumptions that (1) the coarse aggregates are incompressible compared with the porous soft matrix during loading, and (2) the particle density of fines is the same as that of coarse aggregates. Since the fines originate from disintegration of parent rock aggregates, this assumption is reasonable.

The volume fraction of coarse aggregates during oedometer loading can be computed by Eq. (4), and its evolution is shown in Fig. 4. As the void ratio decreases, the volume fraction of aggregates increases with increasing stress level according to Eq. (4). This is consistent with of change of the volume fraction of aggregates in Fig. 4. Note that, the change of volume fraction of aggregates is lower than 0.02, which is negligible within the tested stress levels. In the sequel, the volume fraction is treated as a constant during the compression and shearing process. Note that the change of volume fraction can not be neglected if the matrix undergoes a large deformation, e.g., at extremely high stress level, or the matrix is a soft clay slurry. However, if the volume fraction of phases is incorporated into the sequel analysis, it is also applicable to gap-graded soils with a considerable deformation.

The overall mobilized stress ratio of the gap-graded soils μ_σ is defined as

$$\mu_\sigma = \frac{\tau}{\sigma'} \tag{5}$$

where σ' and τ are the overall vertical stress and overall shear stress of the gap-graded soils, respectively. Note that the stresses are calculated using the initial cross area according to ASTM-3080. Therefore, the vertical stress is marked as a constant. Since the vertical stress and the shear stress are calculated using the same cross area, the stress ratio is irrelevant to the cross area. The stress field is nonuniform, as the stress in aggregates is higher than that of in fine matrix (Lielens et al., 1998; de Boer, 2006; Shi et al., 2020). The stress variables in Eq. (5) are defined as volume average values.

The relationship between overall mobilized stress ratio and overall horizontal shear strain for the gap-graded soils with various coarse fraction is shown in Fig. 5. The overall stress ratio of mixtures shows a relative smooth change at low coarse fractions (below 55%). For the samples with a high coarse fraction, there is an oscillation at a large displacement when the sample shows a constant volume state. This is consistent with the results after previous researches (Li et al., 2013; Wei et al., 2018). The mobilized stress ratio of coarse-fine

mixtures relies on the roughness of the shear surface. DEM simulations reveal that the coarse-fine mixtures exhibits a relative uniform distribution of contact force chains at low coarse fractions. At high coarse fractions, the contact force chains become nonuniform and concentrated between the coarse aggregates (Xu et al., 2019). This may lead to collapse and rearrangement of aggregates in vicinity of the shear plane (Wei et al., 2018). As a result, the overall shear stress shows an oscillation, especially at large strains. The curve shows strain-hardening behavior for the samples with a lower coarse fraction (0%, 20% and 40%) and strain softening behavior for pure aggregates (or specimens with a high coarse fraction at low stress levels). For a given overall shear strain within the prefailure range, the mobilized stress ratio increases with coarse fraction, except for the one with a coarse fraction of 80%. Similar phenomenon was also reported by previous researchers that the mobilized stress ratio of gap-graded specimens with a coarse fraction of ca. 80% is lower than that with smaller coarse fractions (e.g., Vallejo and Mawby, 2000; Elkady *et al*., 2015; Wei *et al.*, 2018). This can be interpreted by the macro-pores within the inter-aggregate apace. As shown in Fig. 3, the black aggregate may move towards the macro-voids due to loss of constraints from the surrounding fines, this suggests an increase of the degree of freedom of coarse aggregates.

It is well recognized that the strain along the vertical profile of specimens is nonuniform. DEM simulations (Zhang *et al*., 2018) show that the strain is concentrated in vicinity of the shear plane. For a complementary qualitative analysis, the vertical strain is calculated from the displacement of the loading cap. The vertical deformation of the gap-graded soils with various coarse fraction is plotted in Fig. 5 in terms of the overall vertical strain and overall horizontal shear strain. The maximum dilation angle is also computed and summarized in Table. 2. It is seen that the pure fine matrix and the gap-graded soil with 20% coarse fraction show volume contraction during the shear process. The shear dilatancy become more significant as the coarse fraction increases, which coincides with the evolution of mobilized

stress ratio. As reported by Monkul and Ozden (2007), the overall behavior is mainly controlled by the fine matrix, until it is reduced to the "transition fines content" ($\phi_m = 1 - \phi_a$ =0.49). The coarse fraction is below "transition coarse content" for the specimens with coarse fractions of 73%. However, it still shows granular-like behavior with a distinctive shear dilatancy. This phenomenon can be interpreted by the densified clay layer between coarse aggregates. The stiffer layer acts like a bridge between adjacent coarse aggregates, which contributes to formation of a granular-like structure (Jafari and Shafiee 2004; Shi et al., 2019). With a further increase of the coarse fraction, volume contraction is suppressed, and shear-induced contraction prevails.

4. A simple model for the mobilized stress ratio

If the gap-graded soils are simplified as a mixture of fines and coarse aggregates, the overall behavior of mixtures reinforced by stiff inclusions can be analyzed within mixture theory. The overall mobilized stress ratio relies on both the inter-aggregate skeleton and that of the soil matrix. Correspondingly, the following is addressed for modelling mobilized stress ratio of gap-graded soils: (1) the change of mobilized stress ratio of the fine matrix, and (2) the evolution of inter-granular structure during shearing process.

The coarse fraction ψ_a is constant during mechanical loading. Therefore, it is not suitable for describing the change of inter-aggregate structure, especially for very soft matrix e.g., sand-bentonite mixtures which shows a large deformation. As reported by Tandon and Weng (1988), the volume average concept provides satisfactory descriptions of the behavior of gap-graded geomaterials. The volume fraction ϕ_a is a state variable, relying on the void ratio. Therefore, it is used for homogenizing state variables of binary gap-graded soils, and the relationship between the overall strain and the value of matrix is

$$\varepsilon_h = (1-\phi_a)\varepsilon_{h,m} \tag{6}$$

where ε_h is overall horizontal shear strain of gap-graded soils, and $\varepsilon_{h,m}$ is the horizontal shear strain of the matrix. They are correlated using the volume fraction of sand aggregate. It should be noted that the fines cannot fully fill the inter-aggregate space for an extremely high fraction of aggregates (e.g., 80% in this study), leading to macro-pores in the gap-graded soils. In this case, Eq. (4) is not applicable.

The mobilized stress ratio of fine matrix $\mu_{\sigma,m}$ is defined as

$$\mu_{\sigma,m} = \frac{\tau_m}{\sigma'_m} \tag{7}$$

where σ'_m and τ_m are the vertical stress and shear stress of the matrix, respectively. Both are defined as volume average values. However, the mobilized stress ratio of fine matrix cannot be computed from its definition, since the local stresses cannot be measured in direct shear tests. The change of mobilized stress ratio of pure sand is essentially dependent of vertical stress levels. A hyperbolic function is adopted to correlate the mobilized stress ratio and the horizontal shear strain of the fine matrix:

$$\mu_{\sigma,m} = \frac{\varepsilon_{h,m}}{a + b\varepsilon_{h,m}} \tag{8}$$

where *a* and *b* are model parameters for the fine matrix. The vertical stress does not show significant change during the shearing process. Therefore, the slope of tangent in Fig. 5 resembles the tangent stiffness of the mixtures. The hyperbolic function is successful in simulating decrease of stiffness and asymptotic state of various geomaterials (Duncan and Chang, 1970; Yin, 1999a; Chong and Santamarina, 2016; Nagula et al., 2018). The test data and regression curve are presented in Fig. 6 in terms of the relationship between $\varepsilon_{h,m}/\mu_{\sigma,m}$ and $\varepsilon_{h,m}$, revealing an excellent regression with a correlation coefficient of 0.99.

To model the mobilized stress ratio within mixture theory, it is assumed that the inter-

aggregate space is fully filled with the fine matrix. This corresponds to the weathered soils due to intense disintegration of weak rocks. As shown in Fig. 2, macro-pores prevail between the aggregates when the coarse fraction is higher than 73%. Therefore, only the specimens with a coarse fraction less than 73% (0%, 20%, 40%, 55%) can be treated based on the homogenization theory. The initial porosity of the fine matrix is the same as that of the pure fine soil, therefore, it is reasonable to assume that the change of mobilized stress ratio of the matrix in gap-graded soils follows the one of the pure fine soil (Eq. 8). Substitution of Eq. (6) into Eq. (8) gives:

$$\mu_{\sigma,m} = \frac{\varepsilon_h}{a(1-\phi_a) + b\varepsilon_h} \tag{9}$$

The mobilized stress ratio of the matrix can be estimated from the volume fraction of aggregates and the overall horizontal strain. To create a bridge between the mobilized stress ratio of matrix and the overall value, a structure variable η is introduced. It is defined as the ratio of the overall mobilized stress ratio and the mobilized stress ratio of the fine matrix:

$$\eta = \frac{\mu_\sigma}{\mu_{\sigma,m}} \tag{10}$$

Fig. 7 illustrates the change of structure variable η against the overall horizontal shear strain. The structure variable decreases with the overall horizontal shear strain during the shearing process, which becomes approximately constant beyond 9.0% of the overall shear strain. The structure variable appears to be rather independent of the vertical stress level, although there is some scatter at initial shearing stage. To reduce the oscillation of test data, average value of the structure variable at three different stress levels is taken. The results of gap-graded soils with three different coarse fractions are summarized in Fig. 8. It is seen that the structure variable is affected by both the coarse fraction and the horizontal shear strain. The data points move upwards as the coarse fraction increases. After being replotted in double logarithmic plot, $\ln\eta$ changes almost linearly with $\ln\varepsilon_h$:

$$\eta = \exp(\beta - \alpha \ln \varepsilon_h) \tag{11}$$

where α and β are structure variables which seems independent of overall horizontal shear strain during shearing process. At a given overall shear strain, substitution of Eqs. (9) and (11) into Eq. (10) gives

$$\mu_\sigma = \frac{\exp(\beta - \alpha \ln \varepsilon_h)\varepsilon_h}{a(1-\phi_a) + b\varepsilon_h} \tag{12}$$

The structure variables for the gap-graded soils with various coarse fractions are calibrated using regression analysis as given in Table 3. It is seen that both two variables increase nonlinearly with the increase of coarse fraction. There are two limit cases for the structure variables (α and β) of gap-graded soils. The overall mobilized stress ratio should equal the one of the matrix in case of a negligible coarse fraction ($\phi_a \approx 0$), i.e., η=1, and $\alpha = \beta$=0. When the fines fraction equals the minimum porosity of the pure coarse aggregates, the overall void ratio approaches the minimum value (the lowest point in the ideal compaction line in Fig. 2). The corresponding volume fraction of the aggregates $\bar{\phi}_a$ is given as

$$\bar{\phi}_a = \frac{1}{1+e_{\min,a}} \tag{13}$$

An inter-aggregate structure forms at the densest packing state of gap-graded soils, which overtakes additional external loading. Note that the stiffness of the inter-granular structure in gap-graded soils should be much higher than the one with pure aggregates: For granular specimens with pure aggregates, fracturing and collapse of load-bearing aggregates induces a rearrangement of the structure (Pestana and Whittle, 1995; McDowell 2002; McDowell and Harireche 2002; Mesri and Vardhanabhuti, 2009). This induces a remarkable decrease of the stiffness. On the contrary, the inter-aggregate space in gap-graded soils is filled with a matrix (0%, 20%, 40% and 55% coarse fraction in this study). The stress in coarse aggregates is relatively uniform due to the confining stress provided by the surrounding matrix. This

decreases the possibility of splitting and fracturing of coarse aggregates and prevents further rearrangement of inter-aggregate structure (Zhang and Baudet, 2013). Consequently, the inter-granular structure for gap-graded soils is much more stable than the one with pure aggregates, and the structure variables (α and β) should be extremely high at the densest packing state.

Based on the above discussions, the structure variables can be expressed as follows:

$$\alpha = \left(\frac{\bar{\phi}_a}{\bar{\phi}_a - \phi_a} \right)^{\xi_1} - 1 \tag{14a}$$

$$\beta = \left(\frac{\bar{\phi}_a}{\bar{\phi}_a - \phi_a} \right)^{\xi_2} - 1 \tag{14b}$$

where ξ_1 and ξ_2 are structure parameters which controls the sensitivity of structure variables (α and β) on the coarse fraction. Since the structure parameters relie on the evolution of inter-aggregate skeleton, they depend on shape and size distribution of coarse particles (Herle and Gudehus, 1999).

The basic structure of gap-graded mixture is characterized by the size ratio between large and small particles, and the coarse fraction. Both the effect of coarse fraction and particle size ratio (between coarse and fine particles) is considered in the proposed model. The coarse fraction effect is explicitly incorporated into Eq. (14). According to mixture theory, no matter what the particle size ratio is, the mechanism governing the overall behavior of gap-graded soils is the same (Ueda et al., 2011; Zhou et al., 2016). The effect of particle size ratio (between coarse and fine particles) on the deformation behavior of gap-graded soils is implicitly incorporated into the model by means of the structure variables in Eq. 14. The structure variables, α and β, decrease as the particle size ratio falls, and they reduce to 0 if the particle size of the fines and aggregates is the same.

5. Validation of the proposed model

The proposed model has four parameters: a, b, ξ_1 and ξ_2. a and b are for the mobilized stress ratio of the fine matrix, ξ_1 and ξ_2 are structure parameters correlated with the change of inter-aggregate structure with increasing coarse fraction. Only two direct shear tests are required for calibrating the mentioned model parameters: one on pure fine matrix, and the other on gap-graded soil with a predefined coarse fraction. a and b can be calibrated from the relationship between mobilized stress ratio and horizontal shear strain of fine matrix. The structure parameters α and β can be calibrated by trial and error procedure through a direct shear test on a gap-graded specimen. Experimental data of two gap-graded soils are used for validating the model: soil-sand mixtures in this work, and the sand-gravel mixtures from literature (Vallejo *et al*., 2014).

Gap-graded soils in this work

The gap-graded soils in this work is a mixture of coarse sand material and fine sandy soils, with fine sandy soils being the matrix and the coarse material being the inclusions. The proposed model is evaluated in this section by comparing simulations with the test data of the mixtures. Calibration of the model parameters are shown in Figs. 6, 9 and 10, and the value of parameters are listed in Table 4. To distinguish the data between different stress levels, the results are presented in terms of overall shear stress and overall horizontal shear strain. The simulated curves for the gap-graded soils with various fractions are shown in Fig. 11, together with the experimental results (ψ_a =0%, 20%, 40%, 55%, and 80%).

In this work, we focus on gap-graded soils with matrix-sustained structure. As shown in Figs. 11 and 12, the model can well capture the change of stress ratio in direct shear test with coarse fraction below the transitional value. However, the model predictions deviate from the test data with a coarse fraction beyond 73% for the Chongqing soils. This is due to prevailing

macro-voids within inter-aggregated space beyond the transitional coarse fraction (Fig. 3), and the emerging macro-voids reduce the stiffness and shear strength of the gap-graded soils. As a result, the model based on mixture theory is not applicable anymore. As been reported by other researchers, the coarse fraction is usually beyond the transitional value for sandy marine deposits and gap-graded soils in intensely weathered areas (Zhao et al., 2007; Cui et al., 2017; Chen et al., 2020c). Therefore, gap-graded granular soils usually have a matrix-sustained structure, and their behavior can be well reproduced using the proposed model.

Gap-graded soils from literature

Two granular materials are used for producing gap-graded soils by Vallejo *et al*. (2014): gravel is used as coarse inclusions, and Ottawa sand was used as the matrix. The coefficient of uniformity of Ottawa sand is 1.3, with an average diameter of 0.59 mm. The maximum and minimum void ratios are 0.88 and 0.48, respectively. The average diameter of coarse inclusions is 5 mm. The minimum void ratio of the inclusion is assumed to be 0.60 for the calculation of $\bar{\phi}_a$ in Eq. (13). The particle densities of gravel inclusions and sand matrix are 2.40 Mg/m^3 and 2.65 Mg/m^3, respectively. Gap-graded soils with seven different coarse fractions (from 0% to 30%) were tested by the authors. The initial void ratio of the matrix in the gap-graded specimens are 0.8 regardless of the coarse fractions. Three various fractions, 0%, 15%, and 30%, are used for validation of the model, and the corresponding volume fractions of the inclusions are 0%, 8.9%, and 19.6%, respectively. The specimens were compressed to two desired vertical stresses (52 kPa and 103 kPa) followed by a direct shear process with a displacement rate of 0.02 mm/min. Fig. 12 presents a comparison of the experimental data with model predictions of the sand-gravel mixtures, suggesting that the model can represent the coarse fraction effect on mobilized shear strength in direct shear tests.

6. Conclusions

A simple model has been proposed for describing the evolution of mobilized stress ratio, and its validation is presented using the experimental data in this study and data from literature. Conclusions are summarized as follows:

(1) The initial overall void ratio of the binary soils initially decreases approximately linearly with the coarse fraction. With a further increase of the coarse fraction, the initial overall porosity increases, and the mobilized stress ratio decreases due to arising macro-pores within the inter-aggregates space.

(2) The change of inter-aggregates skeleton is considered by introducing a structure variable. It increases with volume fraction of coarse aggregates and decreases approximately linearly with the overall horizontal shear strain in double logarithmic plot.

(3) The model has four parameters which can be easily calibrated from two direct shear tests on pure matrix and gap-graded soils, respectively. The model reproduces well the evolution of mobilized stress ratio of the gap-gaped soils in this work and those from the literature.

Appendix-1

There are two types of structure according to the coarse fraction, matrix-sustained structure and aggregate-sustained structure. In this study, we deal with the matrix-sustained structure, and the structure of the fine matrix is relatively uniform without macro-voids (Fig. 3). Therefore, volume of voids in mixtures can be well represented by the volume of voids in fine matrix, and the overall deformation of gap-graded mixtures relies on the decrease of volume of voids in fines. The mixture can be divided into three parts: (1) the solid phase of fine matrix (denoted as V_{sm}), (2) the volume of voids in fine matrix (denoted as V_{vm}), and (3) the

volume of coarse aggregates (denoted as V_a). Suppose that the volume of solid phase of fine matrix is one unit (i.e., V_{sm} =1). The volume of voids in fine matrix is

$$V_{vm} = e_m \tag{15}$$

Where e_m is the void ratio of fine matrix. From the definition of the void ratio of aggregates e_a,

$$V_a = \frac{V_{sm} + V_{vm}}{e_a} = \frac{1 + e_m}{e_a} \tag{16}$$

Hence, the coarse fraction and overall void ratio at the transitional point can be derived according to its definition:

$$\tilde{\psi}_a = \frac{V_a}{V_{sm} + V_a} = \frac{1 + e_m}{1 + e_m + e_{\min,a}} \tag{17}$$

$$\tilde{e} = \frac{V_{vm}}{V_{sm} + V_a} = \frac{e_m e_{\min,a}}{1 + e_m + e_{\min,a}} \tag{18}$$

The overall void ratio can be derived according to its definition:

$$e = \frac{V_{vm}}{V_{sm} + V_a} = \frac{e_m}{1 + V_a} \tag{19}$$

The dry mass of the fines m_s and aggregates m_a are

$$m_s = \rho_s V_{sm};\ m_a = \rho_a V_a \tag{20}$$

Suppose that the density of fines and aggregates are the same, the coarse fraction is derived as:

$$\psi_a = \frac{m_a}{m_s + m_a} = \frac{\rho_a V_a}{\rho_s V_{sm} + \rho_a V_a} = \frac{V_a}{1 + V_a} \tag{21}$$

The following equations can be derived from Eq. (19) and Eq. (21):

$$e_m = \frac{e}{1 - \psi_a};\ V_a = \frac{\psi_a}{1 - \psi_a} \tag{22}$$

The volume fraction of aggregates is defined as:

$$\phi_a = \frac{V_a}{V_{sm} + V_{vm} + V_a} = \frac{V_a}{1 + e_m + V_a} \tag{23}$$

Substitution of Eq. (22) into Eq. (23), it gives:

$$\phi_a = \frac{\psi_a}{1+e} \tag{24}$$

List of symbols

a, b	Model parameters for the fine matrix
C_u	Coefficient of uniformity
C_c	Coefficient of curvature
D_{50}	Diameters at 50 percentiles in PSD curve
e	Overall void ratio
e_a	Void ratio of coarse aggregates.
e_m	Void ratio of fines
e_{min}	Overall minimum void ratio
$e_{min,a}$	Minimum void ratio of coarse aggregates
$e_{max,a}$	Maximum void ratio of coarse aggregates
m_s	Dry mass of fine matrix
m_a	Dry mass of coarse aggregates
V_a	Volume of coarse aggregates
V_{sm}	Volume of solid phase in fine matrix
V_{vm}	Volume of void phase in fine matrix
α, β	Structure variables
ε_h	Overall horizontal shear strain
$\varepsilon_{h,m}$	Horizontal shear strain of matrix
ε_v	Overall vertical strain
η	Structure variable
μ_σ	Overall mobilized stress ratio

$\mu_{\sigma,m}$	Mobilized stress ratio of matrix
ξ_1, ξ_2	Structure parameters
ρ_a	Density of aggregates
ρ_s	Density of fine particles
σ'	Overall vertical stress
σ'_m	Vertical stress of matrix
τ	Overall shear stress
τ_m	Shear stress of matrix
ϕ_a	Volume fraction of coarse aggregates
$\bar{\phi}_a$	The maximum packing density of coarse aggregates
ψ_a	Coarse fraction

Acknowledgments

This study was partially supported by the National Natural Science Foundation of China (under Grant No. 51908193) and the Fundamental Research Funds for the Central Universities (Grant No. B200201050; B200204032). The work in this paper is also supported three GRF projects (Grant No. 16201419; PolyU 152209/17E; PolyU 152179/18E), a Research Impact Fund (RIF) project (R5037-18), all from Research Grants Council (RGC) of Hong Kong Special Administrative Region Government (HKSARG) of China. The authors also acknowledge the financial supports from Research Institute for Sustainable Urban Development of The Hong Kong Polytechnic University, grants (BBAG, ZDBS, ZVNC) from The Hong Kong Polytechnic University.

References

Bolton, M. D., Lam, S. Y., & Osman, A. S. (2008). Supporting excavations in clay–from analysis to decision-making. In *Geotechnical Aspects of Underground Construction in Soft Ground* (pp. 31-44). CRC Press.

Bolton, M. D., Powrie, W. and Symons, I. F. (1990a). The design of stiff in-situ walls retaining over-consolidated clay part 1, short term behavior. *Ground Engineering*, 23(1): 34-39.

Bolton, M. D., Powrie, W. and Symons, I. F. (1990b). The design of stiff in-situ walls retaining over-consolidated clay part 2, short term behavior. *Ground Engineering*, 23(2): 22-28.

Chang, C. S., Meidani, M., & Deng, Y. (2017). A compression model for sand-silt mixtures based on the concept of active and inactive voids. *Acta Geotechnica*, 12(6), 1301-1317.

Chang, C. S., & Yin, Z. Y. (2011). Micromechanical modeling for behavior of silty sand with influence of fine content. *International Journal of Solids and Structures*, 48(19), 2655-2667.

Chang, W. J., Chang, C. W., & Zeng, J. K. (2014). Liquefaction characteristics of gap-graded gravelly soils in K_0 condition. *Soil Dynamics and Earthquake Engineering*, 56, 74-85.

Chandler, R. J. (2000). The Third Glossop Lecture: Clay sediments in depositional basins: the geotechnical cycle. *Quarterly Journal of Engineering Geology and Hydrogeology*, 33(1), 7-39.

Chen, W. B., Feng, W. Q., Yin, J. H., Chen, J. M., Borana, L., & Chen, R. P. (2020a). New model for predicting permanent strain of granular materials in embankment subjected to low cyclic loadings. *Journal of Geotechnical and Geoenvironmental Engineering*, 146(9), 04020084.

Chen, W. B., Liu, K., Feng, W. Q., Borana, L., & Yin, J. H. (2020b). Influence of matric suction on nonlinear time-dependent compression behavior of a granular fill material. *Acta*

Geotechnica, 15(3), 615-633.

Chen, W. B., Liu, K., Yin, Z. Y., & Yin, J. H. (2020c). Crushing and flooding effects on one-dimensional time-dependent behaviors of a granular soil. *International Journal of Geomechanics*, 20(2), 04019156.

Chong, S. H., & Santamarina, J. C. (2016). Soil compressibility models for a wide stress range. *Journal of Geotechnical and Geoenvironmental Engineering*, 142(6), 06016003.

Cui, Y. F., Zhou, X., & Guo, C. X. (2017). Experimental study on the moving characteristics of fine grains in wide grading unconsolidated soil under heavy rainfall. *Journal of Mountain Science*, 14(3), 417-431.

De Boer, R. (2006). Trends in continuum mechanics of porous media (Vol. 18). *Springer Science & Business Media*.

De Boer, R., & Ehlers, W. (1986). On the problem of fluid and gas-filled elasto-plastic solids. *International journal of solids and structures*, 22(11), 1231-1242.

Duncan, J. M., & Chang, C. Y. (1970). Nonlinear analysis of stress and strain in soils. *Journal of Soil Mechanics & Foundations Div*. 96, 1629-1653.

Goudarzy, M., König, D., & Schanz, T. (2016). Small strain stiffness of granular materials containing fines. *Soils and Foundations*, 56(5), 756-764.

Guo, C. X., Cui, Y. F. (2020) Pore structure characteristics of debris flow source material in the Wenchuan earthquake area. *Engineering Geology*, 267:105499.

Herle, I., & Gudehus, G. (1999). Determination of parameters of a hypoplastic constitutive model from properties of grain assemblies. *Mechanics of Cohesive-frictional Materials*, 4(5), 461-486.

Hong, Z., Zeng, L. L., Cui, Y. J., Cai, Y. Q., & Lin, C. (2012). Compression behaviour of natural and reconstituted clays. *Géotechnique*, 62(4), 291-301.

Jafari, M. K., & Shafiee, A. (2004). Mechanical behavior of compacted composite clays.

Canadian Geotechnical Journal, 41(6), 1152-1167.

Kumar, G. V., & Wood, D. M. (1999). Fall cone and compression tests on clay±gravel mixtures. *Géotechnique*, 49(6), 727-739.

Li, Y., Huang, R., Chan, L. S., & Chen, J. (2013). Effects of particle shape on shear strength of clay-gravel mixture. *KSCE Journal of Civil Engineering*, 17(4), 712-717.

Lielens, G., Pirotte, P., Couniot, A., Dupret, F., & Keunings, R. (1998). Prediction of thermo-mechanical properties for compression moulded composites. *Composites Part A: Applied Science and Manufacturing*, 29(1-2), 63-70.

Meng Q. X., Wang H. L., Xu W. Y., et al. (2019) Multiscale strength reduction method for heterogeneous slope using hierarchical FEM/DEM modeling. *Computers and Geotechnics*, 115:103164.

Mesri, G., & Vardhanabhuti, B. (2009). Compression of granular materials. *Canadian Geotechnical Journal*, 46(4), 369-392.

Monkul, M. M., & Ozden, G. (2007). Compressional behavior of clayey sand and transition fines content. *Engineering Geology*, 89(3), 195-205.

Nagula, S. S., Robinson, R. G., & Krishnan, J. M. (2018). Mechanical characterization of pavement granular materials using hardening soil model. *International Journal of Geomechanics*, 18(12), 04018157.

Osman, A. S. and Bolton, M. D. (2004). A new design method for retaining walls in clay. *Canadian Geotechnical Journal*, 41(3): 451-466.

Osman A. S. and Bolton M. D. (2006). Design of braced excavations to limit ground movements. Proceedings of Institution of Civil Engineers, *Geotechnical Engineering*, 159 (3): 167-175.

Peng, D., Xu, Q., Liu, F., He, Y., Zhang, S., Qi, X., ... & Zhang, X. (2018). Distribution and failure modes of the landslides in Heitai terrace, China. *Engineering Geology*, 236, 97-110.

Pestana, J. M., & Whittle, A. J. (1995). Compression model for cohesionless soils. *Géotechnique*, 45(4), 611-631.

Peters, J. F., & Berney IV, E. S. (2010). Percolation threshold of sand-clay binary mixtures. *Journal of Geotechnical and Geoenvironmental Engineering*, 136(2), 310-318.

Qin, C. B., & Chian, S. C. (2017). Kinematic analysis of seismic slope stability with a discretisation technique and pseudo-dynamic approach: a new perspective. *Géotechnique*, 68(6), 492-503.

Ruggeri, P., Segato, D., Fruzzetti, V. M. E., & Scarpelli, G. (2016). Evaluating the shear strength of a natural heterogeneous soil using reconstituted mixtures. *Géotechnique*, 66(11), 941-946.

Shi, X. S., & Herle, I. (2017). Numerical simulation of lumpy soils using a hypoplastic model. *Acta Geotechnica*, 12(2), 349-363.

Shi, X. S., Nie, J., Zhao, J., & Gao, Y. (2020). A homogenization equation for the small strain stiffness of gap-graded granular materials. *Computers and Geotechnics*, 121, 103440.

Shi, X. S., & Yin, J. (2017). Experimental and theoretical investigation on the compression behavior of sand-marine clay mixtures within homogenization framework. *Computers and Geotechnics*, 90, 14-26.

Shi, X. S., & Yin, J. (2018). Consolidation behavior for saturated sand-marine clay mixtures considering the intergranular structure evolution. *Journal of Engineering Mechanics*, 144(2), 04017166.

Shi, X. S., Zhao, J., Yin, J., & Yu, Z. (2019). An elastoplastic model for gap-graded soils based on homogenization theory. *International Journal of Solids and Structures*. 163, 1-14.

Shin, H., & Santamarina, J. C. (2012). Role of particle angularity on the mechanical behavior of granular mixtures. *Journal of Geotechnical and Geoenvironmental Engineering*, 139(2), 353-355.

Simoni, A., & Houlsby, G. T. (2006). The direct shear strength and dilatancy of sand–gravel mixtures. *Geotechnical and Geological Engineering*, 24(3), 523.

Tan, D. Y., Yin, J. H., Feng, W. Q., Zhu, Z. H., Qin, J. Q., & Chen, W. B. (2019). New Simple Method for Calculating impact force on flexible barrier considering partial muddy debris flow passing through. *Journal of Geotechnical and Geoenvironmental Engineering*, 145(9), 04019051.

Tandon, G. P., & Weng, G. J. (1988). A theory of particle-reinforced plasticity. *Journal of Applied Mechanics*, 55(1), 126-135.

Thevanayagam, S., & Martin, G. R. (2002). Liquefaction in silty soils-screening and remediation issues. Soil Dynamics and Earthquake Engineering, 22(9-12), 1035-1042.

Thevanayagam, S., & Mohan, S. (2000). Intergranular state variables and stress-strain behaviour of silty sands. *Géotechnique*, 50(1), 1-23.

Thevanayagam, S., Shenthan, T., Mohan, S., & Liang, J. (2002). Undrained fragility of clean sands, silty sands, and sandy silts. *Journal of Geotechnical and Geoenvironmental Engineering*, 128(10), 849-859.

Ueda, T., Matsushima, T., & Yamada, Y. (2011). Effect of particle size ratio and volume fraction on shear strength of binary granular mixture. *Granular Matter*, 13(6), 731-742.

Vallejo, L. E. (2001). Interpretation of the limits in shear strength in binary granular mixtures. *Canadian Geotechnical Journal*, 38(5), 1097-1104.

Vallejo, L. E., Lobo-Guerrero, S., & Seminsky, L. F. (2014). Shear Strength of Sand-Gravel Mixtures: Laboratory and Theoretical Analysis. Geo-Congress 2014: *Geo-characterization and Modeling for Sustainability* (pp. 74-83).

Vallejo, L. E., & Mawby, R. (2000). Porosity influence on the shear strength of granular material-clay mixtures. *Engineering Geology*, 58(2), 125-136.

Wei, H. Z., Xu, W. J., Xu, X. F., Meng, Q. S., & Wei, C. F. (2018). Mechanical properties of

strongly weathered rock-soil mixtures with different rock block contents. *International Journal of Geomechanics*, 18(5), 04018026.

Xu, D. S., Tang, J. Y., Zou, Y., Rui, R., & Liu, H. B. (2019). Macro and micro investigation of gravel content on simple shear behavior of sand-gravel mixture. *Construction and Building Materials*, 221, 730-744.

Yagiz, S. (2001). Brief note on the influence of shape and percentage of gravel on the shear strength of sand and gravel mixtures. *Bulletin of Engineering Geology and the Environment*, 60(4), 321-323.

Yang, Z. Y., & Juo, J. L. (2001). Interpretation of sieve analysis data using the box-counting method for gravelly cobbles. *Canadian geotechnical journal*, 38(6), 1201-1212.

Yao, Y. P., Hou, W., & Zhou, A. N. (2009). UH model: three-dimensional unified hardening model for overconsolidated clays. *Géotechnique*, 59(5), 451-469.

Yao, Y. P., Sun, D. A., & Luo, T. (2004). A critical state model for sands dependent on stress and density. *International Journal for Numerical and Analytical Methods in Geomechanics*, 28(4), 323-337.

Yin, J. H. (1999a). Non-linear creep of soils in oedometer tests. *Géotechnique*, 49(5), 699-707.

Yin, J. H. (1999b). Properties and behavior of Hong Kong marine deposits with different clay contents. *Canadian Geotechnical Journal*, 36(6), 1085-1095.

Yin, Z. Y., Huang, H. W., & Hicher, P. Y. (2016). Elastoplastic modeling of sand-silt mixtures. *Soils and Foundations*, 56(3), 520-532.

Yin, Z. Y., Zhao, J., & Hicher, P. Y. (2014). A micromechanics-based model for sand-silt mixtures. *International Journal of Solids and Structures*, 51(6), 1350-1363.

Zhang, Z., Cui, Y., Chan, D. H., & Taslagyan, K. A. (2018). DEM simulation of shear vibrational fluidization of granular material. *Granular Matter*, 20(4), 71.

Zhao, M. H., Zou, X. J., & Zou, P. X. (2007). Disintegration characteristics of red sandstone

and its filling methods for highway roadbed and embankment. *Journal of Materials in Civil Engineering*, 19(5), 404-410.

Zhou, W., Xu, K., Ma, G., Yang, L., & Chang, X. (2016). Effects of particle size ratio on the macro-and microscopic behaviors of binary mixtures at the maximum packing efficiency state. *Granular Matter*, 18(4), 81.

Zhou, W. H., Garg, A., & Garg, A. (2016). Study of the volumetric water content based on density, suction and initial water content. *Measurement*, 94, 531-537.

List of Tables

Table 1: Basic physical properties of the fine matrix and coarse aggregates

Materials	Density of soil particles (Mg/m^3)	Sand (%)	Silts (%)	Clay (%)	Particle size distribution		
					D_{50}	C_c	C_u
Fine matrix	2.73	89	9	2	0.19	2.41	5.31
Coarse aggregates	2.63	100	0	0	1.49	0.97	1.32

Table 2: Maximum dilation angle for gap-graded soils with various stress levels and coarse fractions

Stress level (kPa)	ψ_a=0%	ψ_a=20%	ψ_a=40%	ψ_a=55%	ψ_a=80%	ψ_a=100%
157	-1.6°	0.0°	8.3°	26.9°	21.0°	43.2°
314	-3.4°	0.0°	6.7°	23.7°	11.7°	32.8°
451	-3.5°	-1.5°	3.1°	22.5°	7.7°	29.7°

Table 3: Values of structure variables for the gap-graded soils with various coarse fractions

Parameters	ψ_a=0%	ψ_a=20%	ψ_a=40%	ψ_a=55%
α	0	0.065	0.138	0.336
β	0	0.128	0.362	0.985

Table 4: Parameters of the proposed model for the gap-graded soils

Sources	a	b	ξ_1	ξ_2
	(%)	---	---	---
This study	5.25	1.04	0.24	0.57
Vallejo *et al*., 2014	1.06	0.30	0.45	0.90

List of Figures

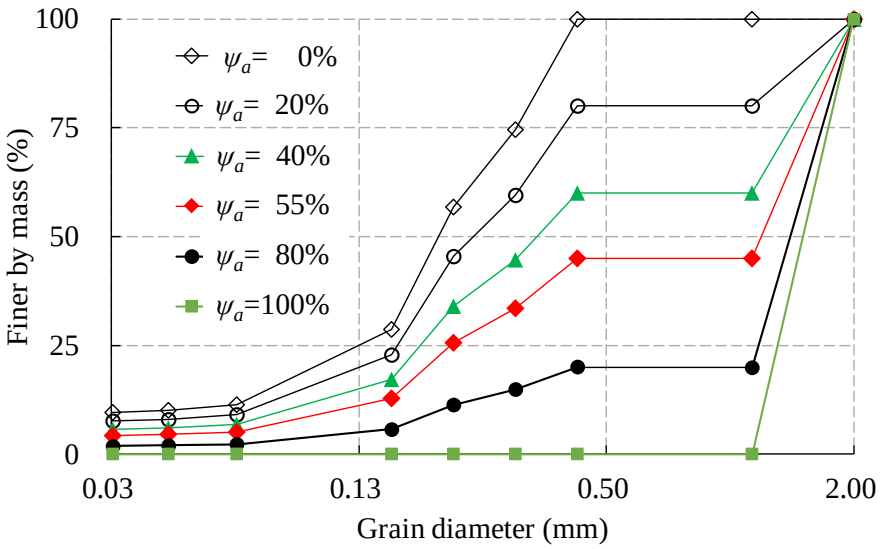

Figure 1: Particle size distribution of the tested gap-graded soil with different coarse fraction

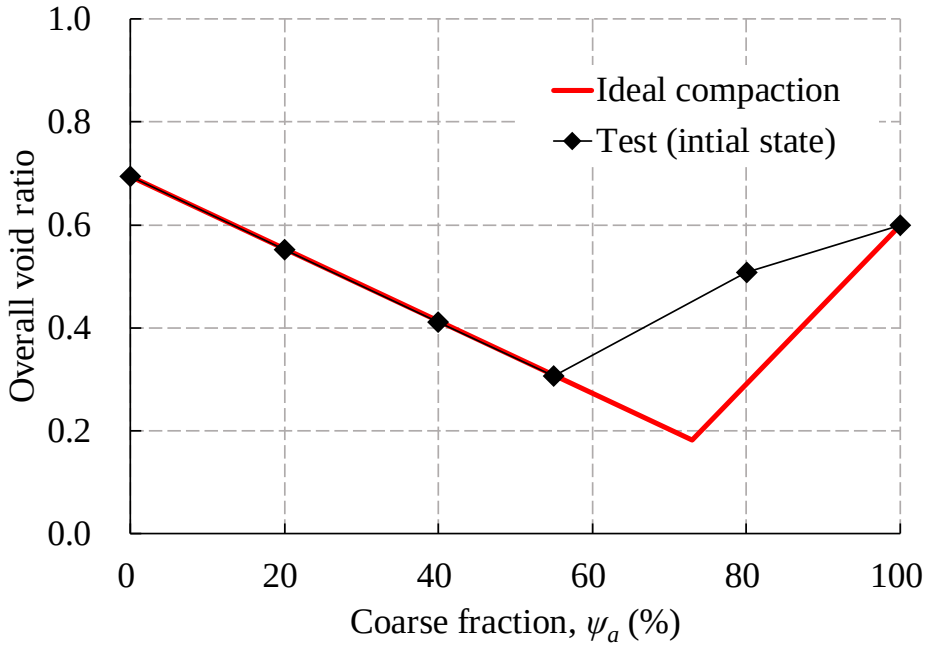

Figure 2: Change of initial void ratio with mass fraction of coarse aggregates

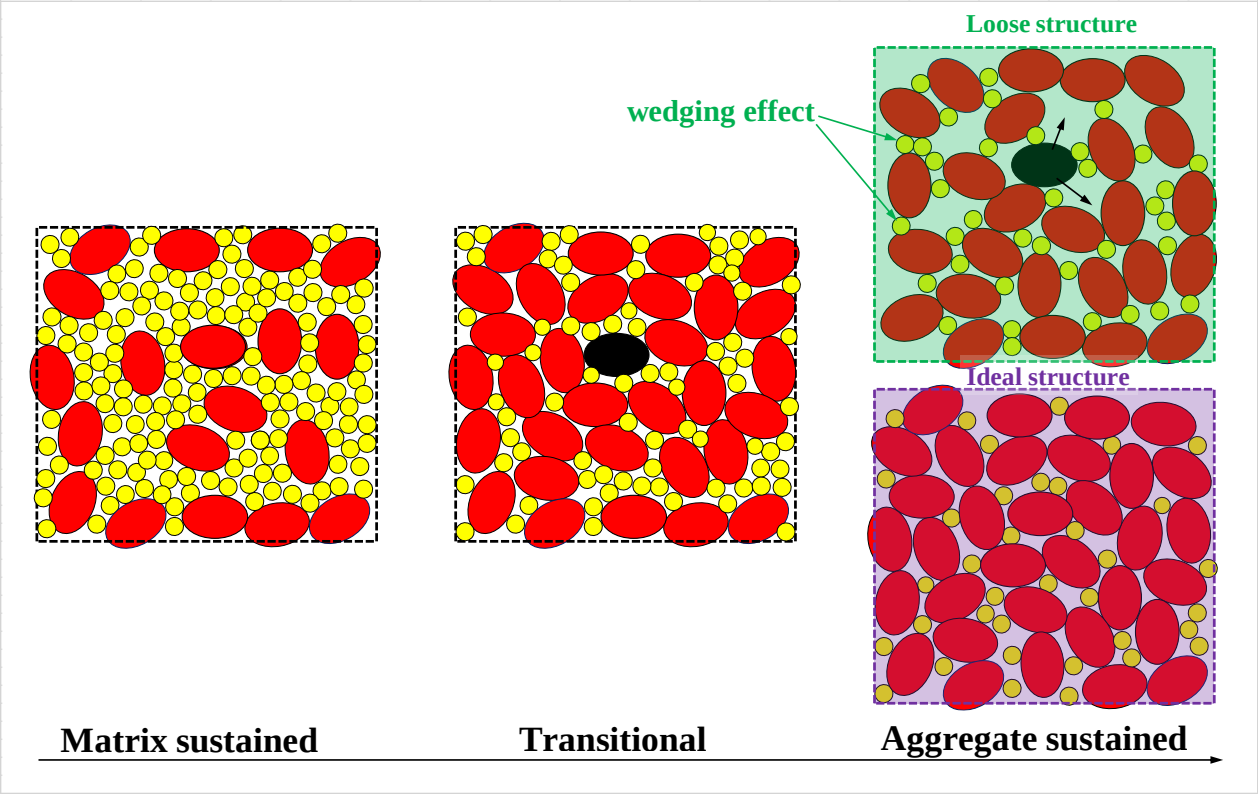

Figure 3: Soil structure with various coarse fractions considering the wedging effect (Goudarzy *et al*., 2016)

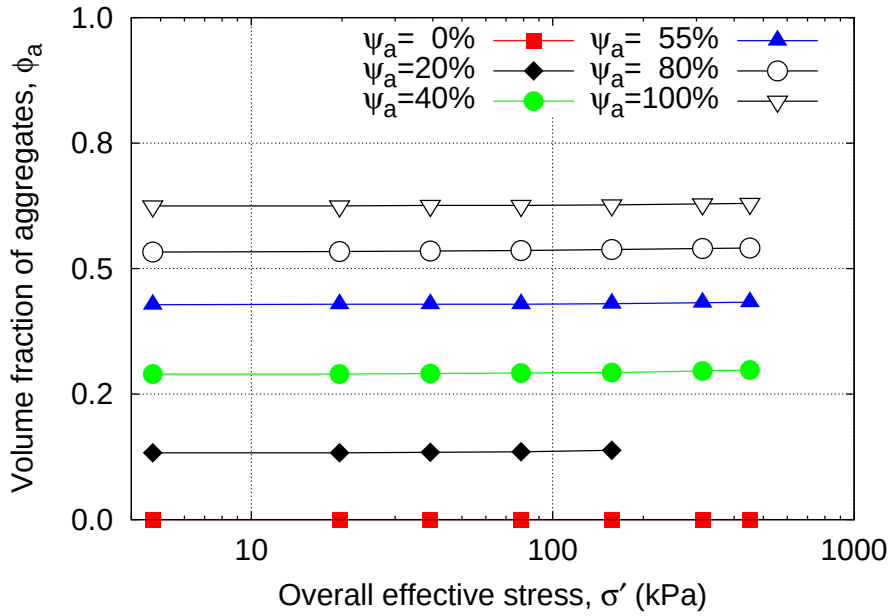

Figure 4: Change of volume fraction of coarse aggregates in the gap-graded soils

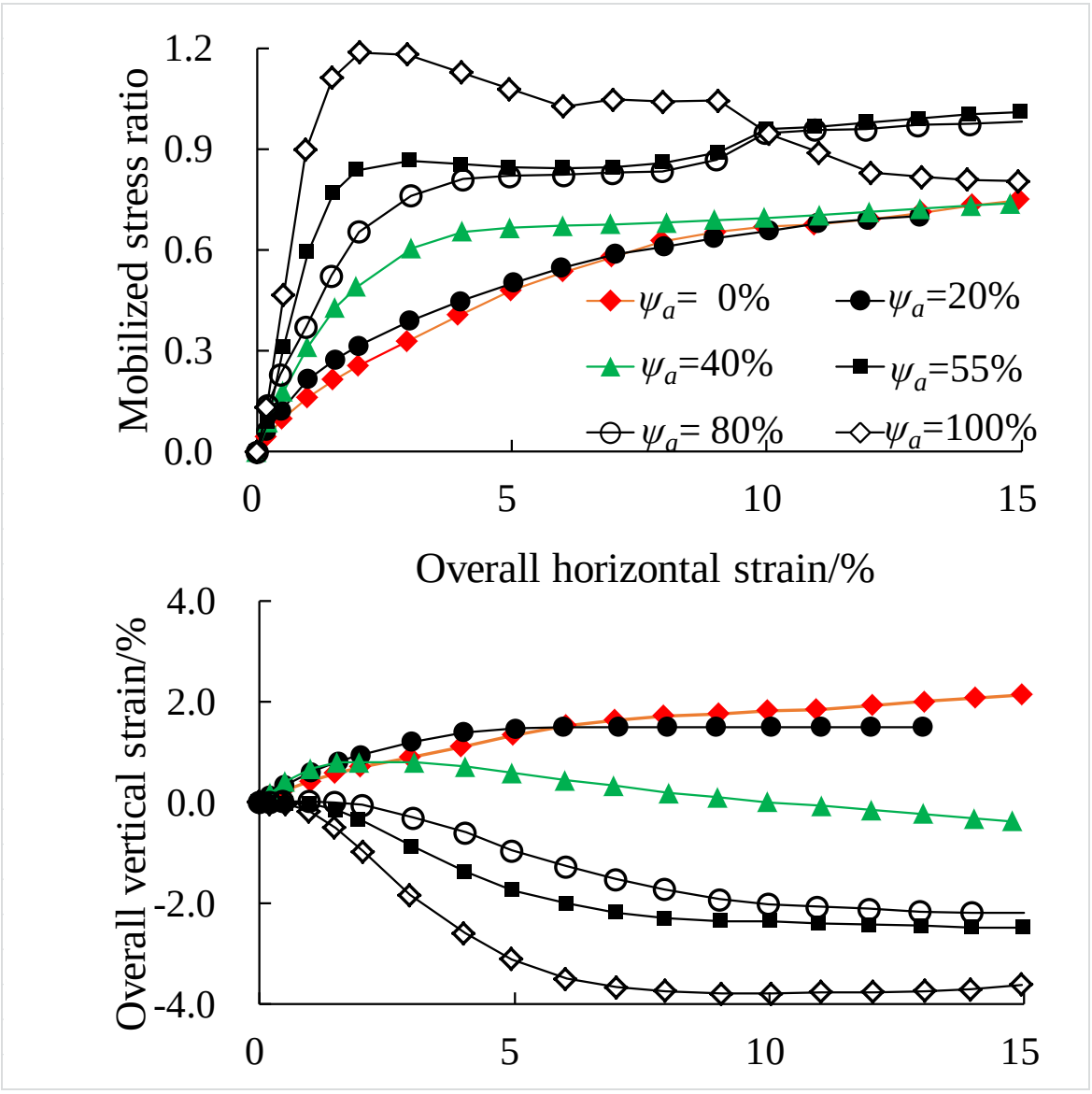

(a) σ'=157 kPa

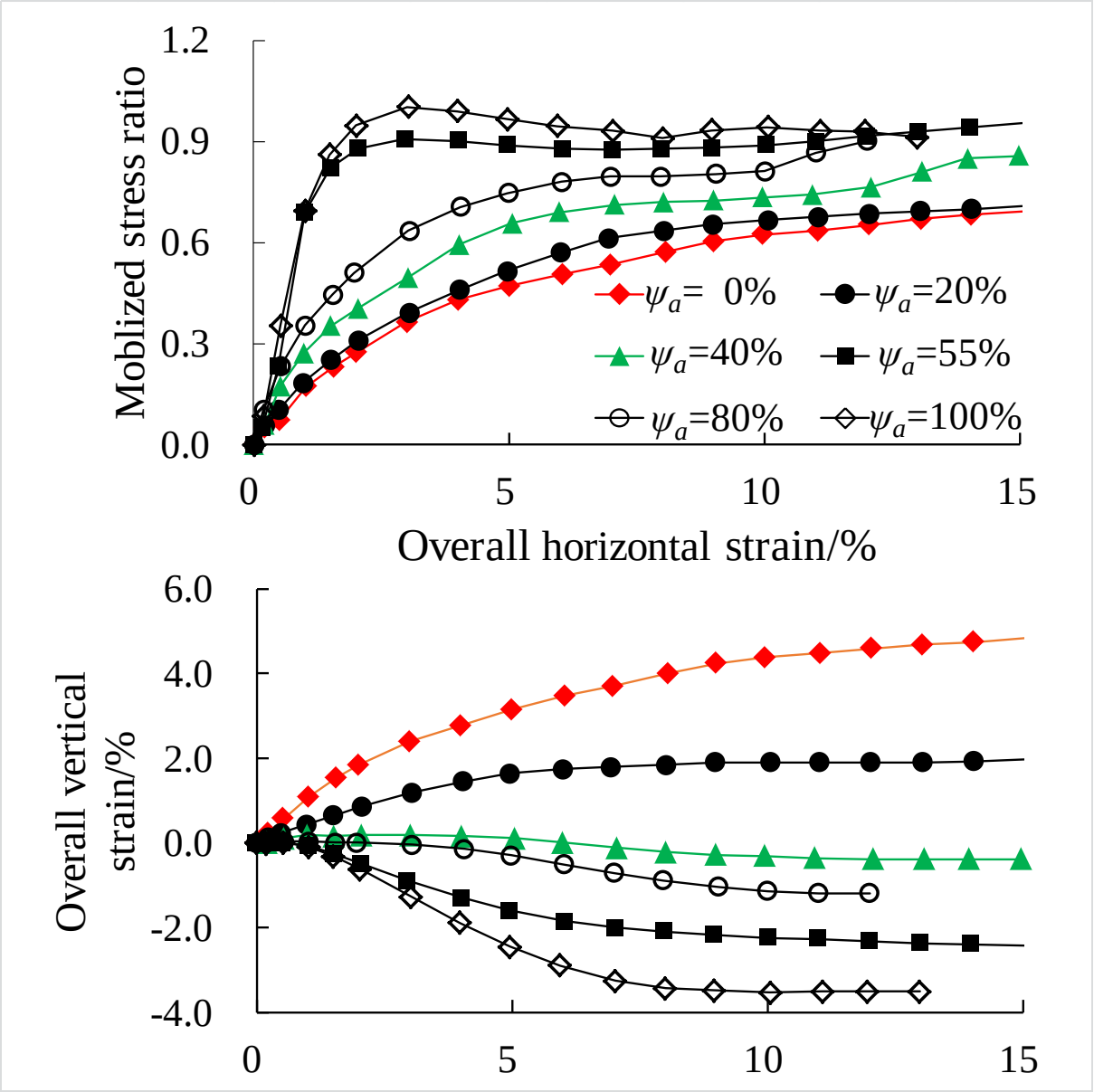

(b) σ'=314 kPa

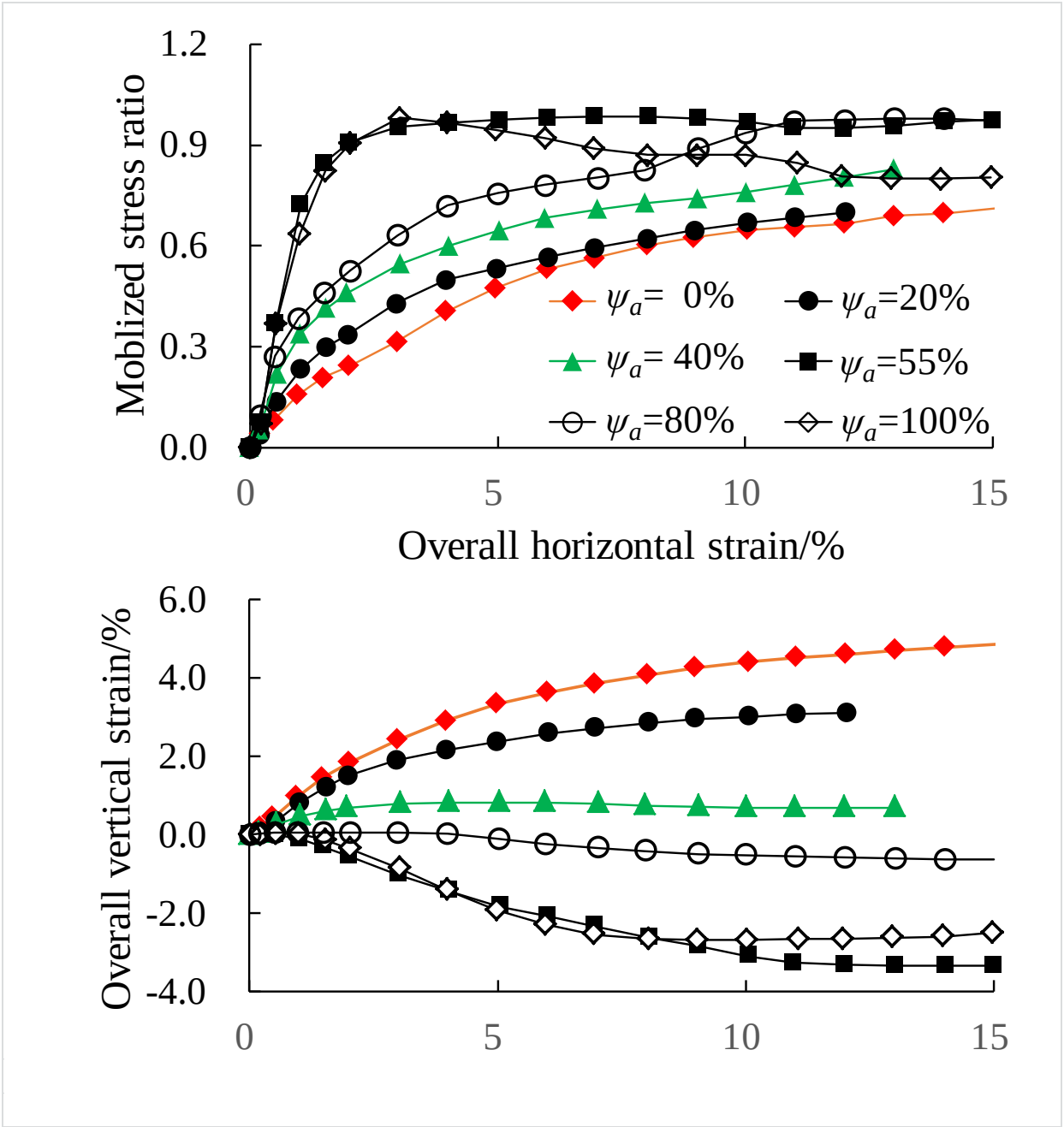

(c) σ'=451 kPa

Figure 5: Change of mobilized stress ratio and overall vertical strain for the gap graded soils with various coarse fractions

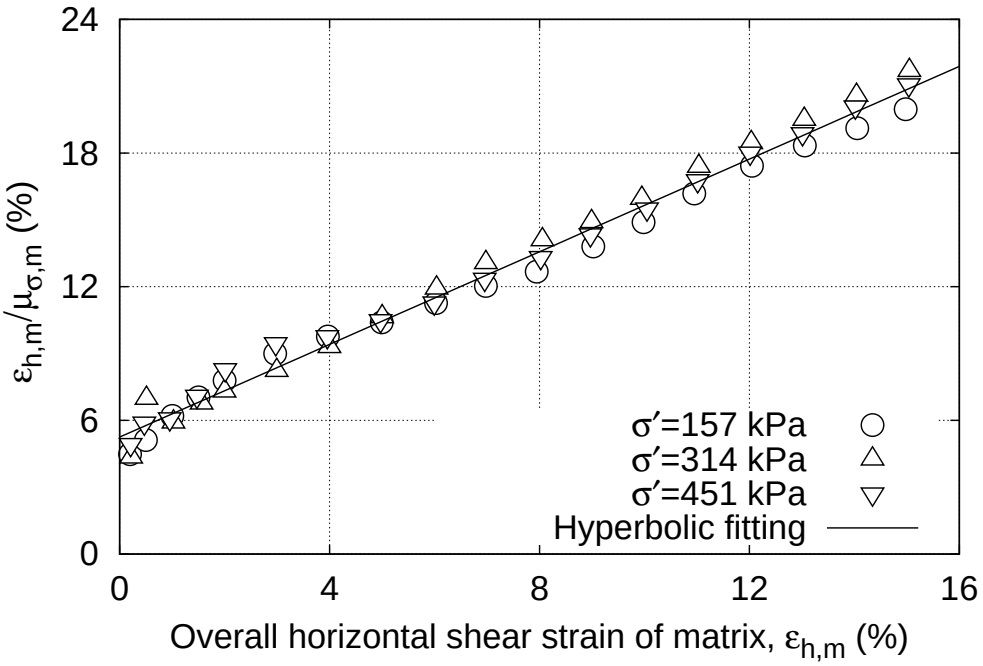

Figure 6: Correlation between the mobilized stress ratio and the overall horizontal shear strain for pure fine matrix

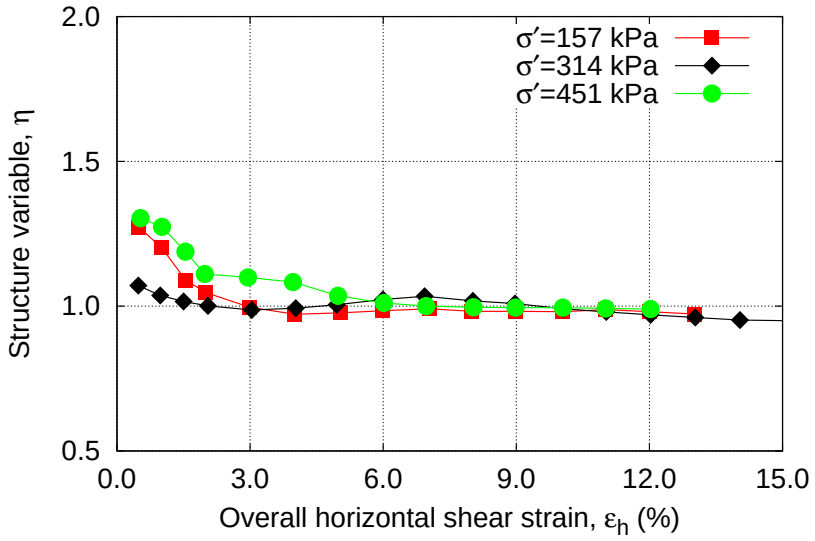

(a) $\psi_a = 20$ %

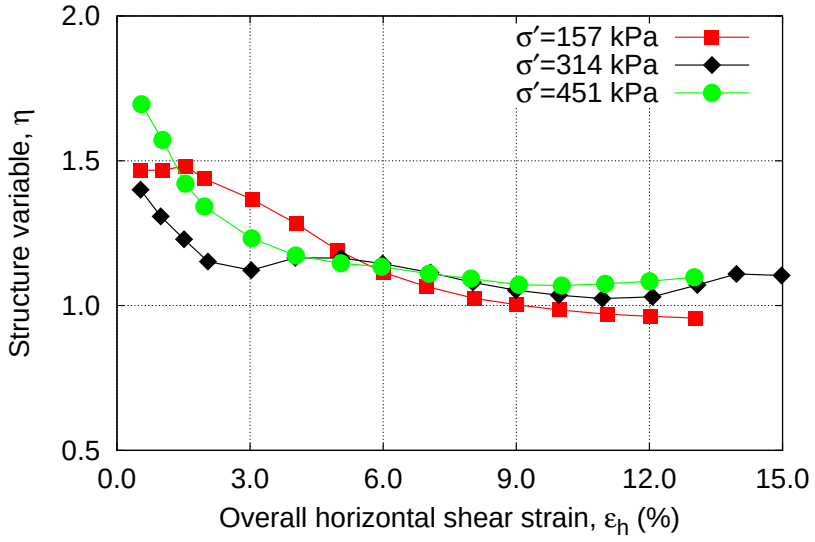

(b) $\psi_a = 40$ %

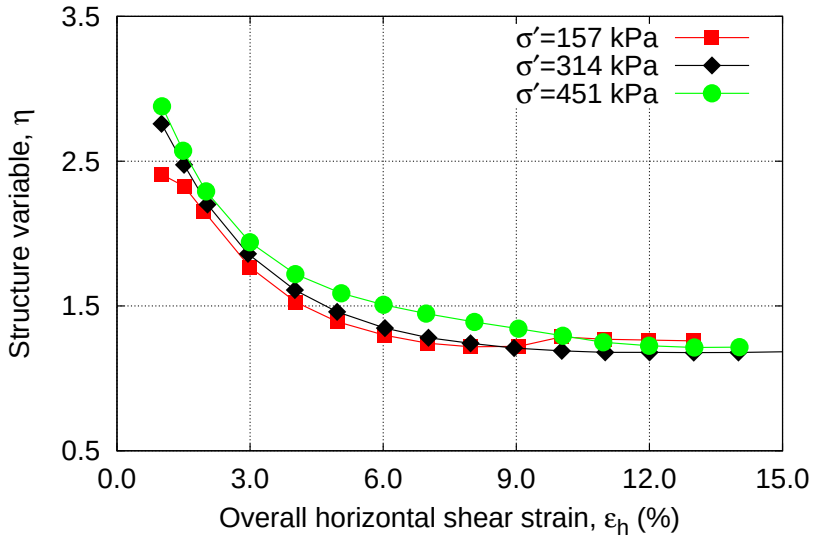

(c) $\psi_a = 55$ %

Figure 7: Evolution of the structure variable η with overall horizontal shear strain

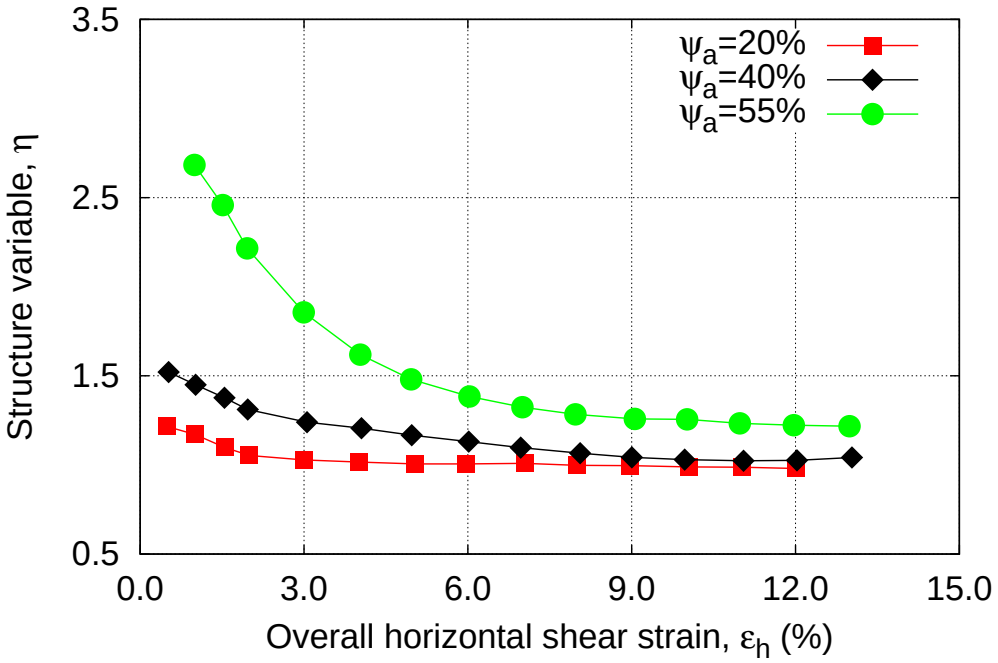

Figure 8: Change of average value of the structure variable η with overall horizontal shear strain

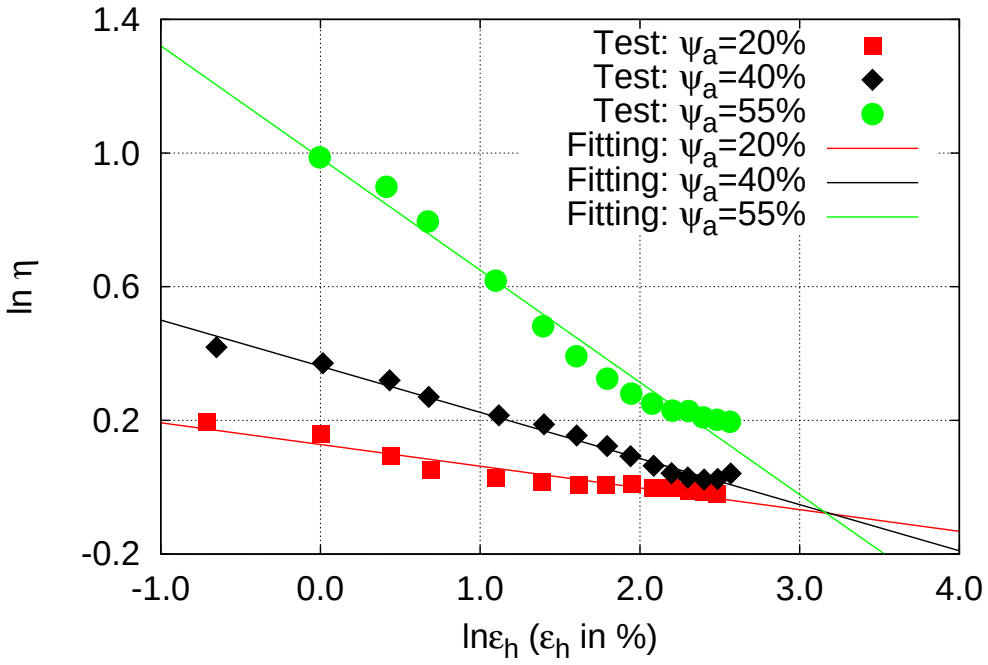

Figure 9: Relationship between logarithms of the structure variable η and overall horizontal shear strain

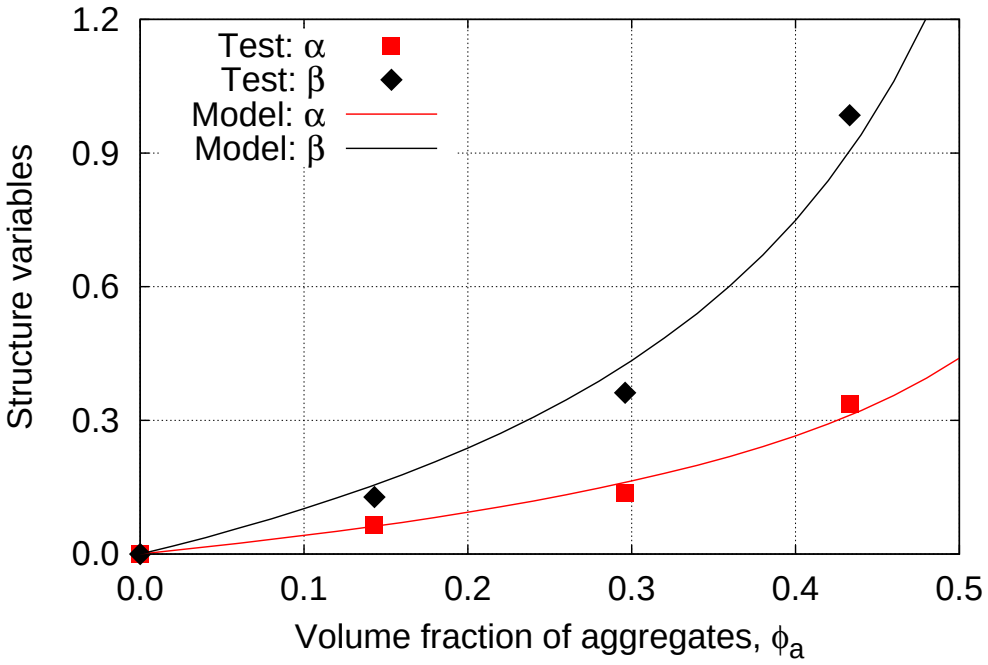

Figure 10: Change of structure variables with volume fraction of coarse aggregates

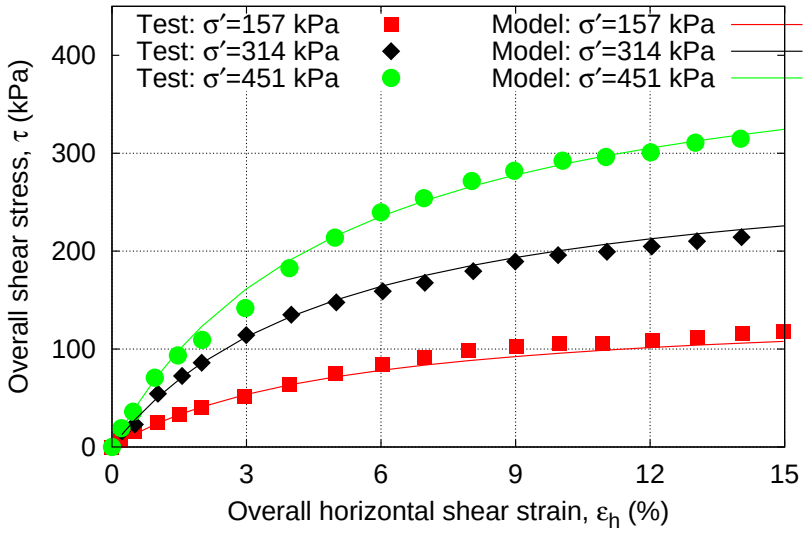

(a) $\psi_a = 0$ %

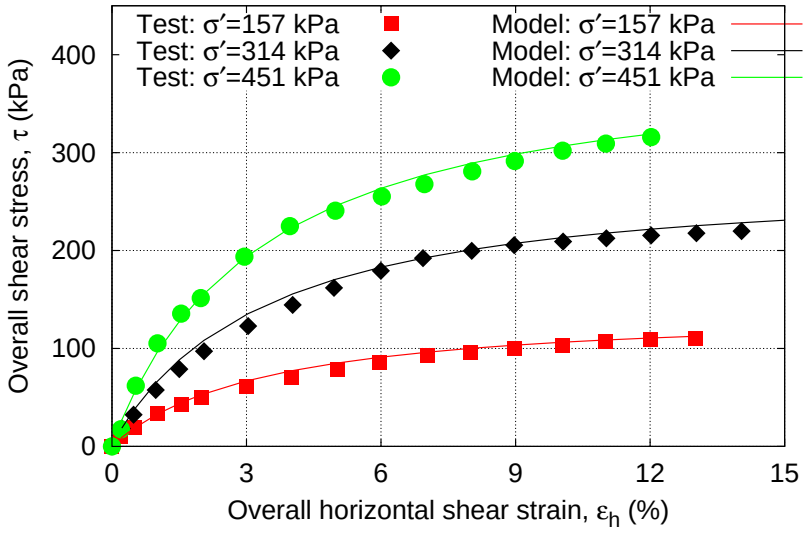

(b) $\psi_a = 20$ %

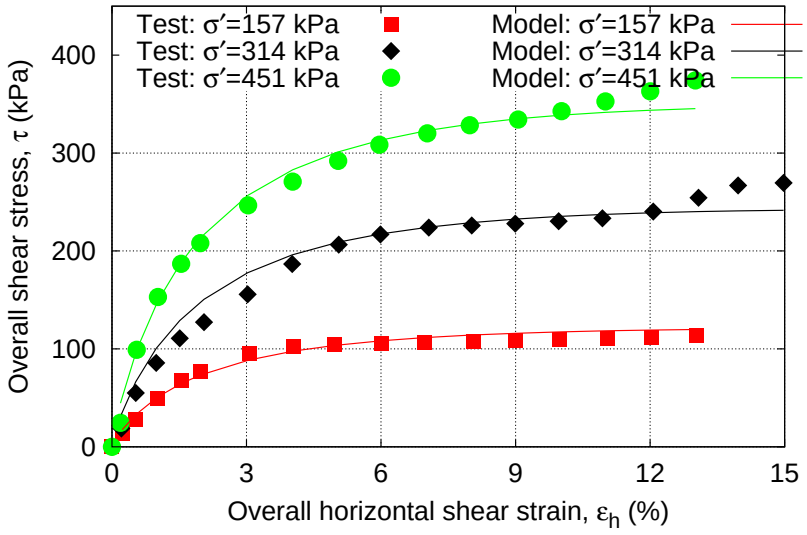

(c) $\psi_a = 40$ %

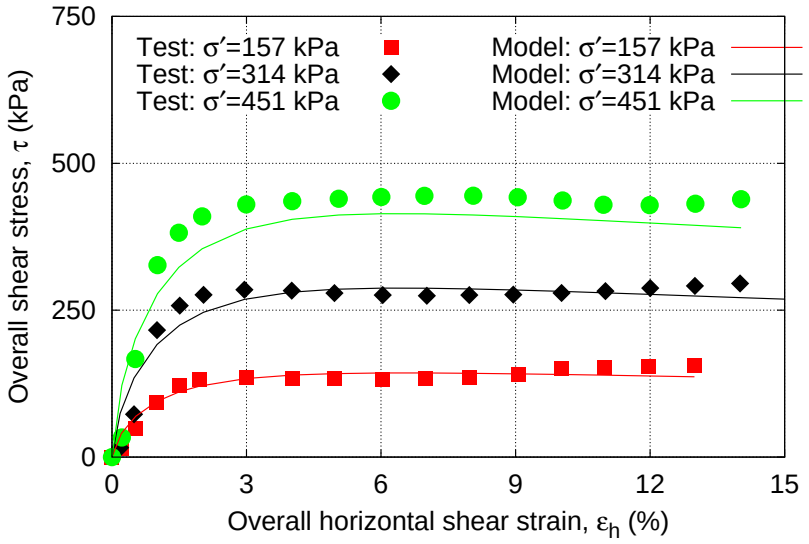

(d) $\psi_a = 55$ %

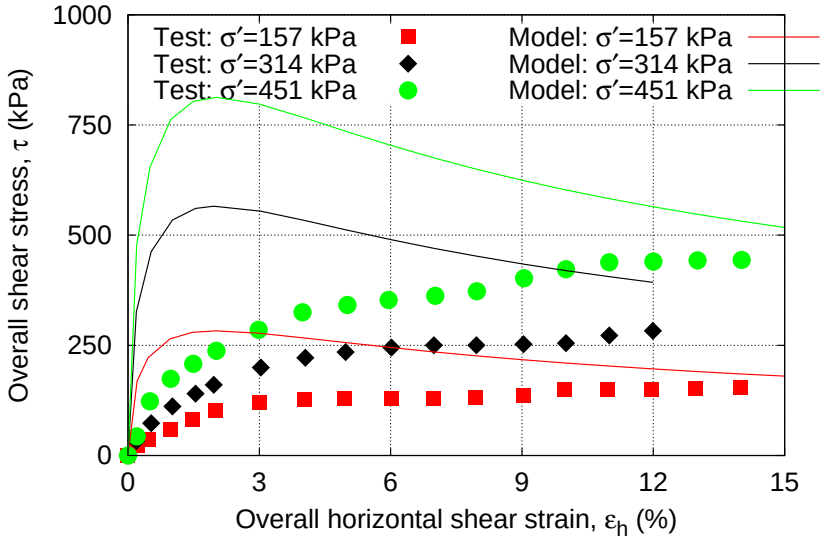

(e) $\psi_a = 80$ %

Figure 11: Comparison between experimental data and model simulation

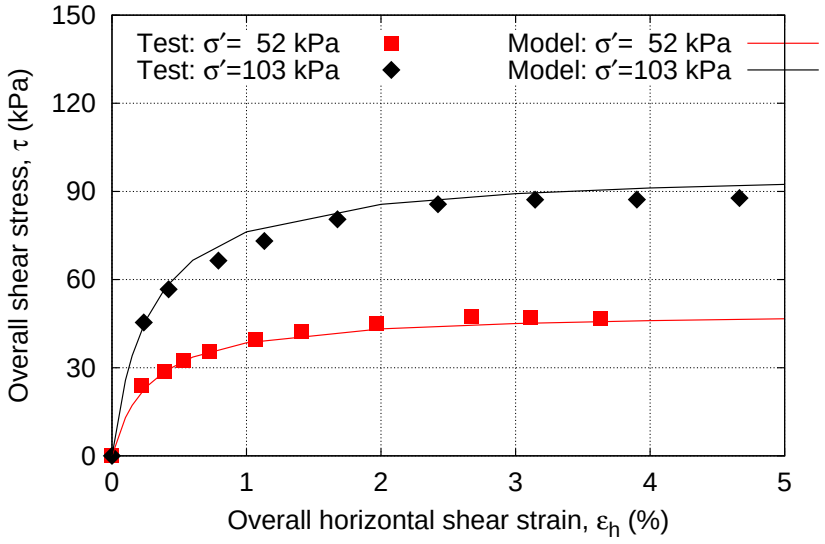

(a) $\psi_a = 0$ %

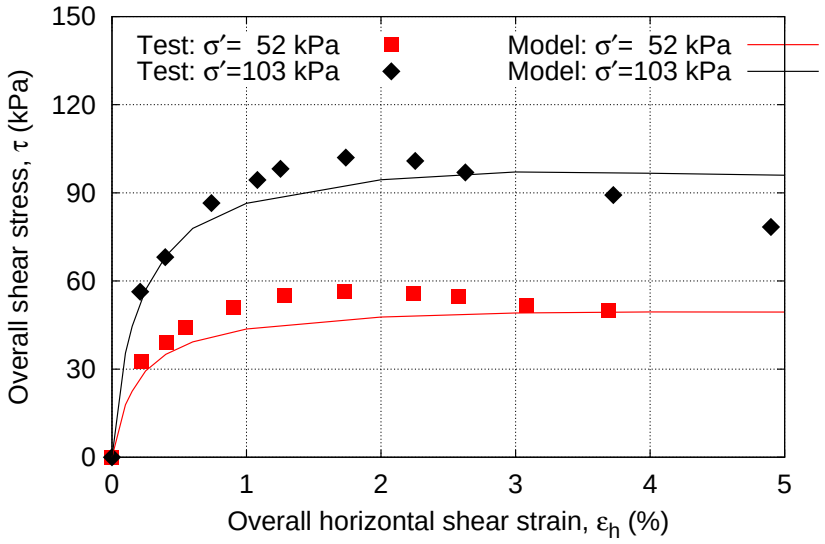

(b) $\psi_a = 15$ %

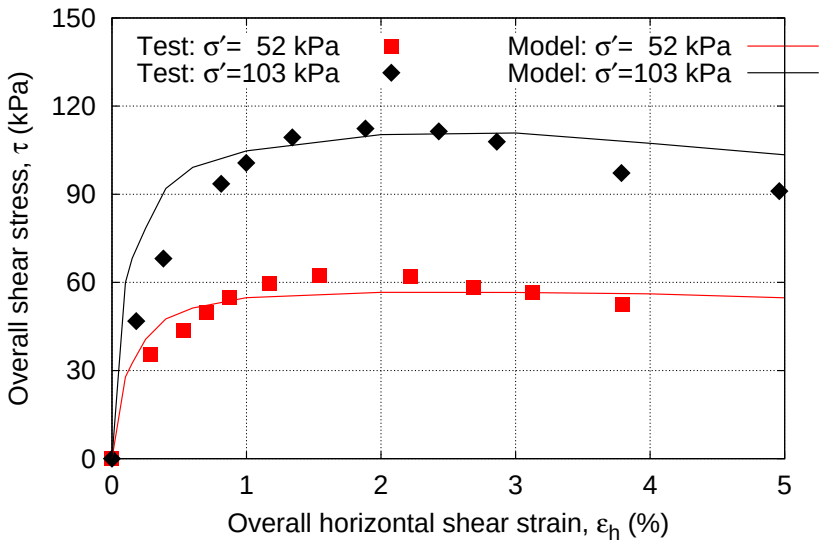

(c) $\psi_a = 30$ %

Figure 12: Comparison between experimental data and model simulation (test data from Vallejo *et al*., 2014)